TU Delft

Delft University of Technology

Rolling-horizon electric vertical takeoff and landing arrival scheduling for on-demand urban air mobility

Kleinbekman, Imke; Mitici, Mihaela; Wei, Peng

DOI
10.2514/1.I010776

Publication date
2019

Document Version
Accepted author manuscript

Published in
Journal of Aerospace Information Systems (online)

Citation (APA)
Kleinbekman, I., Mitici, M., & Wei, P. (2019). Rolling-horizon electric vertical takeoff and landing arrival scheduling for on-demand urban air mobility. *Journal of Aerospace Information Systems (online)*, *17 (2020)*(3), 150-159. Advance online publication. https://doi.org/10.2514/1.I010776

Important note
To cite this publication, please use the final published version (if applicable).
Please check the document version above.

Copyright
Other than for strictly personal use, it is not permitted to download, forward or distribute the text or part of it, without the consent of the author(s) and/or copyright holder(s), unless the work is under an open content license such as Creative Commons.

Takedown policy
Please contact us and provide details if you believe this document breaches copyrights.
We will remove access to the work immediately and investigate your claim.

This work is downloaded from Delft University of Technology.
For technical reasons the number of authors shown on this cover page is limited to a maximum of 10.

A Rolling-horizon eVTOL Arrival Scheduling for On-demand Urban Air Mobility

Imke C. Kleinbekman * and Mihaela Mitici †
Faculty of Aerospace Engineering, Delft University of Technology, Delft HS 2926, The Netherlands

Peng Wei ‡
Iowa State University, Department of Aerospace Engineering, Ames, IA, 50011, USA

Urban air mobility with electric Vertical Take-Off and Landing (eVTOL) vehicles is envisioned to become a fast and flexible urban transportation mode. Apart from technical challenges for eVTOLs regarding vehicle design and manufacturing, airspace design and traffic control mechanisms are most desired on the operation side. In particular, from an operational point of view, the arrival phase is expected to be the main bottleneck, with restricted vertiport resources, high air traffic density, frequent flight manoeuvres, and limited eVTOL remaining battery energy, all leading to complex operational constraints. This work provides a framework to enable optimal and efficient on-demand eVTOLS arrivals in the context of on-demand urban air mobility. We investigate the throughput of a double landing pad vertiport by proposing a new vertiport terminal area airspace design and a novel rolling-horizon scheduling algorithm with route selection capability to compute the optimal required time of arrival for eVTOLs in a tactical manner. Finally, a case study on arrivals in a hexagonal vertiport network is performed to show the algorithm performance with different configurations. Our simulation results show that up to 50 seconds delay per eVTOL is expected during the commuter peak hours and less than 10 seconds delay is expected during off-peak hours.

I. Introduction

Urban Air Mobility (UAM) with electric Vertical Take-Off and Landing (eVTOL) vehicles is envisioned to become a customised, on-demand air transportation mode, by carrying passengers and cargo safely and efficiently within urban areas. As cities and streets become more congested, UAM offers the potential for significant commute time savings compared to ground transportation modes.

Companies such as Airbus, Bell, Embraer, Joby Aviation, Kitty Hawk, Pipistrel, Volocopter, and Aurora Flight Sciences have been designing, building and testing innovative electric vertical take-off and landing (eVTOL) aircraft for

*Msc Student, Department of Control and Operations, Kluyverweg 1.
†Assistant professor, Department of Control and Operations, Kluyverweg 1.
‡Assistant professor, Department of Aerospace Engineering, 2333 Howe Hall. AIAA Senior Member.

UAM operations [1]. The UAM industry is facing several challenges regarding vehicle design and manufacturing, such as battery technology, assured vehicle autonomy, and scalable manufacturing process. Moreover, in order to make UAM a reliable and practical transportation mode, operational challenges must be addressed. In particular, there is a need for airspace design and air traffic control mechanisms to enable safe and efficient UAM operations with these eVTOL aircraft. In this paper, we focus on solving one particular phase of the UAM operations, i.e. UAM arrivals at a vertiport, by leveraging airspace design/configuration, trajectory optimisation, eVTOL battery modelling and arrival scheduling to support safe and efficient flight operations for on-demand, urban air mobility arrivals.

In contrast to the small drones that can take off and land almost anywhere covered by UTM services, eVTOL vehicles in UAM operations need to take off from and land at specific ground infrastructures called vertiports. A vertiport is an airport for VTOL vehicles. It could range from a single landing pad on top of a parking structure to a larger building with multistory landing pads that could redefine the urban architecture and city planning [2]. When UAM traffic grows, one of the major emerging bottlenecks is expected to be the limited number of vertiports and landing pads. As such, UAM arrivals will become the most safety-critical flight phase due to limited resource of vertiport landing pads, high-density traffic in terminal airspace, frequent flight manoeuvres, and low remaining battery energy for eVTOLs. Therefore, in this paper we propose a suite of mechanisms for tactical UAM arrival management, among which the rolling-horizon arrival scheduling algorithm enables a double landing pad vertiport to land peak hour eVTOLs with less than 50 seconds average delay per aircraft.

The contribution of this paper is two-fold. Firstly, we propose a vertiport terminal area airspace design 13 with a double landing-pad vertiport and multiple arrival routes. Secondly, based on this airspace structure, we develop a rolling-horizon optimisation algorithm that sequences and schedules multiple eVTOLs arriving at the vertiport. Our algorithm extends existing arrival optimisation models designed for commercial aviation [3–5]. The eVTOLs we consider are constrained by their remaining battery energy and their flight performance parameters. Our aim is to minimise the total eVTOL arrival delay at the vertiport. We formulate this problem as a rolling-horizon, mixed-integer linear program. We determine an optimal required time of arrival (RTA) for eVTOLs arriving at the vertiport. These RTAs are the decision variables in our optimisation model, i.e., the required time for the eVTOLs to arrive at the vertiport. Finally, we apply our sequencing and scheduling optimisation algorithm in a case study on arrivals at a hexagonal vertiport network in Houston, TX, USA. The performance of our algorithm is evaluated for different vertiport configurations. Our simulation results show that, during peak hours, at least two landing pads are needed to accommodate the demand. Moreover, we also show that during the peak hours, up to $50s$ delay per eVTOL is expected, while during off-peak hours, less than $10s$ delay per eVTOL is expected.

The remainder of this paper is organised as follows. In Section II we discuss existing literature on eVTOL operations. In Section III we present a model for eVTOLs arrival sequencing and scheduling at a double landing pad vertiport. In Section IV we present sequencing and scheduling results for an EHANG 184 arriving at a double landing pad vertiport.

In Section VI we provide conclusions and recommendations for future work.

II. Related work

Current UAM research efforts are mainly focused on the design of an urban airspace for UAM [2, 6, 7], on UAM demand forecasting [7, 8], and on the design of the vehicles.

One of the most pressing operational challenges for near terminal on-demand UAM operations is the sequencing and scheduling of arrivals since eVTOL flight time is constraint by the remaining life of their electic batteries, the capacity of vertiports is limited, and the operations do not follow a pre-defined arrival schedule. For commercial aviation, where the terminal area exhibits complex arrival trajectories [9], a significant amount of research has addressed the problem of aircraft arrival sequencing and scheduling at an airport [3–5, 10, 11]. However, none of these models consider the remaining flight time as a constraint, as is the case in this paper, where the eVTOL arrivals scheduling problem is restricted by the flight time supported by electric batteries. In fact, research focused on commercial aviation aims at optimising the arrival process by minimizing the fuel consumption [12] or by optimally sequencing the arrival to avoid fuel shortage [13], while the electric battery flights supported by eVTOls pose new battery-related constraints. Various aspects of eVTOL arrival procedures have been investigated in [14, 15]. In [14] an eVTOL vehicle routing, departure and arrival scheduling is developed such that minimum separation is ensured. Here, eVTOL traffic is integrated with existing air traffic. In our previous work [15] we propose an arrival sequencing and scheduling algorithm that minimises eVTOL delay while considering limited battery power and limited, one landing-pad, vertiport capacity.

Existing literature regarding electric battery discharge models for aircraft is limited. In [16–18] battery modelling and predictions for electric winged aircraft are proposed based on flight testing. In these studies, voltage and state of charge profiles are created based on a flight plan using an equivalent circuit model to check if the flight mission can be completed. Since we are not performing flight testing, in this paper we consider a simpler, theoretical battery model [19] that can support eVTOL operations.

This research extends the arrival scheduling models from previous work to a rolling-horizon, eVTOL arrivals sequencing and scheduling at a double landing-pad vertiport. We analyse our proposed model using a 1-day operations demand corresponding to a hexagonal vertiport network in Houston, TX, USA.

III. Model formulation

In this section, we first introduce a generic airspace structure for eVTOL arrivals at a vertiport with 2 landing pads. Next, we propose an optimisation model for a rolling-horizon eVTOL arrivals at a vertiport with 2 landing pads. In doing so, we make use of a flight dynamics model for eVTOLs equipped with one electric battery and a model for the state of charge of an electric battery.

Lastly, we analyse our optimisation model by means of an eVTOL arrival demand model corresponding to a use case

of hexagonal vertiport network in Houston, TX, USA. This use case and its operational concept is described in [20].

In this paper, we only consider eVTOL arrival operations and assume the two landing pads are used for arrivals only. However, our scheduling model is generic and could be extended to departure operations or mixed operations with departures and arrivals. Another operational assumption is continuous descent approach plus a final vertical landing. This consideration is due to operational safety, to avoid vortex ring state, and energy efficiency [21] . Finally, our approach is applicable for other eVTOL aircraft types, as long as new flight dynamics and battery model are provided.

A. Airspace structure for eVTOL arrivals at a vertiport

According to [20, 22, 23] and above assummptions, we consider eVTOLs arriving at a vertiport with 2 landing pads. We assume 2 arrival and 2 departure metering fixes [22] located on a radius r from the vertiport (see Figure 1). The metering fixes are the entrance and exit "gates" to enforce time based separation. The main use of the arrival approach fixes is to funnel traffic and, most importantly, to push the delay absorption to an area with lower traffic density, further away from the vertiport. We note, however, that the geometry in Figure 1, i.e., the location of the approach fixes on the circle of radius r around the vertiport and the values for R and r, do not affect the formulation of the scheduling model, but only the values of the time-to-fly to an approch fix and vertiport, which influence the numerical results of the scheduling model.

Arrivals are initiated on a radius R from the approach fixes. In this paper, we consider only the two arrival fixes, referred to as approach fixes A and B. The distance between the arrival approach fixes is determined as follows. We assume that the final approach area is circular and has a radius of 400m. Then the approach fixes are spaced around the vertiport by a quarter of the final approach area circumference. eVTOLs arriving through fix A (B) land at a corresponding landing pad A (B), independently of the arrivals at the other fix and landing pad. The arrival flow from approach fix A is separated by a distance s from the flow from approach fix B (see Figure 2). Moreover, consecutive arrivals at an approach fix and its corresponding landing pad are separated by Δt_{sep} time units. The flights up to the approach fixes consist of a cruise phase followed by a continuous shallow descent phase (see Figure 2). Continuous shallow descents are selected for energy efficiency and delay absorption [21]. After reaching one of the two approach fixes (see Figure 2), an arriving eVTOL flies a horizontal flight segment of length d, followed by a vertical descent of altitude h.

The structure of the arrival airspace above considers the flight performances of EHANG 184 [23]. Taking into account a possible shallow descent for EHANG 184 up to the approach fixes, we consider $R = 3500m$. We also assume a minimum separation $\Delta t_{sep} = 90s$ between consecutive arrivals to ensure a minimum lateral separation of $1000ft$ or $305m$ [20]. This also avoids that 2 or more eVTOLs are at the same time in the vertical flight phase. Moreover, it ensure that there is sufficient time for landing pad clearance.

The radius $r = 400m$ and $s = 530m$ follow from having $\Delta t_{sep} = 90s$ and an average eVTOL horizontal speed

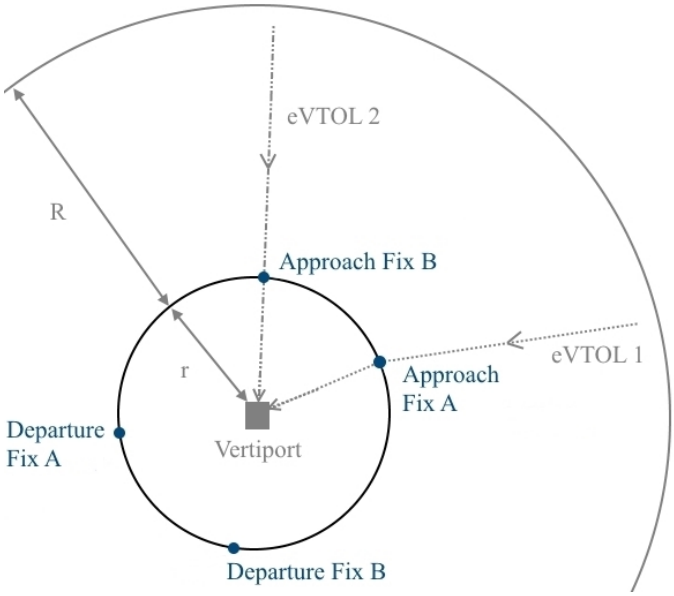

Fig. 1 Airspace structure for eVTOL arrivals at a vertiport with 2 landing pads - top view.

of $5.9m/s$ during the final approach. The distance $d = 135m$ follows from the values assumed for r and s. Lastly, $h = 200m$ allows for a maximum eVTOL shallow descent from a cruise altitude of $500m$ [23] and ensures clearance from high-rise buildings.

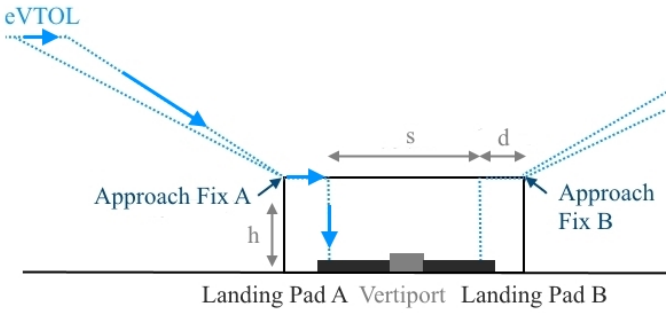

Fig. 2 Airspace structure for eVTOL arrivals at a vertiport with 2 landing pads - side view.

B. eVTOL flight dynamics model

We consider the following flight dynamics model for EHANG 184 multi-rotor eVTOL [23], which is equipped with one electric battery,

$$P_r = P_i + P_a + P_c + P_f = 4 \cdot T \cdot v_i + T \cdot V \cdot \sin\alpha + 0.2 \cdot P_r, \tag{1}$$

$$V = \sqrt{V_x^2 + V_h^2}, \tag{2}$$

$$\alpha = \theta + \gamma = \theta + \arctan\left(\frac{V_x}{V_h}\right), \tag{3}$$

$$v_h = \sqrt{\frac{T_r}{2\rho\pi R^2}}, \tag{4}$$

$$v_i = \frac{v_h^2}{\sqrt{(V \cdot \cos(\alpha))^2 + (V \cdot \sin(\alpha) + v_i)^2}}, \tag{5}$$

where P_r, P_i, P_a, P_c, P_f are the required, induced, parasite, climb and profile power, respectively, with $P_f = 0.2P_r$ [24]. V is the true airspeed with the vertical component V_x and the horizontal component V_h. T, α, θ, γ are the thrust, the angle of attack, the pitch angle and flight path angle, respectively. Also, v_i, v_h, R, T_r, ρ are the induced velocity, the induced velocity in hover, rotor radius, thrust per rotor and the air density, respectively. Here, ρ is assumed to be equal to the international standard atmosphere density at sea level. We further assume that all rotors produce equal thrust. Thus, we assume an upper and lower rotor to produce equal thrust such that $T_r = \frac{1}{8}T$. Lastly, the induced velocity v_i in Eq. (5) follows from momentum theory and the induced velocity in hover, denoted by v_h.

C. Electric battery state-of-charge

We consider the following model for the total electric power demand, P_d, [18, 19]:

$$P_d = SF \cdot \frac{1}{\eta_P}\frac{1}{\eta_e}P_r, \tag{6}$$

where $SF = 1.5$ is a safety factor to account for potential adverse weather conditions and the need for emergency diversion, η_P is the rotor efficiency, $\eta_P = 0.7652$, η_e, is the mechanical efficiency, $\eta_e = 0.85$. We further consider the following model [19] for the battery State of Charge (SOC) demand during a flight phase k that starts at time t_0^k and ends at time t_f^k, $1 \le k \le 4$, where $k = 1$ corresponds to the cruise phase, $k = 2$ corresponds to the shallow descent

phase, $k = 3$ corresponds to the horizontal final approach and $k = 4$ corresponds to the vertical final approach:

$$I(k) = \frac{P_d(k)}{V_n}, \tag{7}$$

$$SOC(k) = \frac{I(k) \cdot \left(t_f^k - t_0^k\right)}{3600 \cdot Q}, \tag{8}$$

$$SOC = \sum_{k=1}^{4} SOC(k), \tag{9}$$

where $I(k)$ is the total current of all battery cells during flight phase k, $1 \leq k \leq 4$, V_n is the nominal battery voltage, Q is the battery capacity. The battery is assumed to be empty if it reaches a 10% SOC, to prevent it from deep discharge. We use this battery model and the flight dynamics model in Section III.B to limit the latest possible landing time RTA_l. This hard constraint ensures that each aircraft lands before its SOC drops below 10%.

D. A rolling-horizon eVTOL arrival sequencing and scheduling at a vertiport

Using the airspace structure in Section III.A, the flight dynamics model for an eVTOL in Section III.B and the eVTOL battery model in Section III.C, in this section we propose an optimal, rolling-horizon sequencing and scheduling algorithm for eVTOL arrivals at a vertiport. We also take into account the possibility for eVTOLs to hover at a distance $R + r$ away from the vertiport. Here, hovering is seen as an additional possibility to impose delay on eVTOLs when the arrival rate is larger than the landing rate of the eVTOLs at the vertiport, i.e., the delay imposed on eVTOLs is too large to be absorbed by means of shallow descent. The objective of this optimisation model is to minimise the total time deviation of arriving eVTOLs from their preferred time of arrival. Next we define the preferred eVTOL times of arrival.

Firstly, given the airspace structure in Section III.A and the eVTOL flight dynamics in Section III.B, we determine, for a given Required Time of Arrival (RTA) at the vertiport, an optimal eVTOL arrival trajectory with respect to energy consumption. These optimal arrival trajectories are computed using the GPOPS-II software [25]. For a given RTA, the output of GPOPS-II is an optimal eVTOL arrival trajectory, which is defined by: the state variables (V_x, V_h, altitude and distance), the control variables (T and θ) and, the total energy required to fulfil the trajectory.

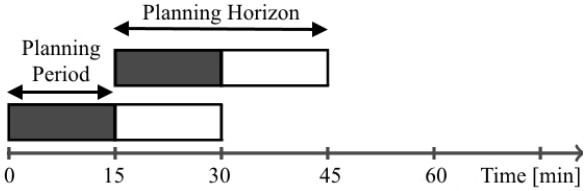

Fig. 3 Rolling-horizon for eVTOL sequencing and scheduling.

Next, we use the GPOPS-II output to determine the required power P_r at each flight phase $k, 1 \leq k \leq 4$, of the eVTOL arrival trajectory (see also Section III.B). Further, P_r is used to determine the battery power demand P_d and the

SOC demand for the eVTOL battery (see Section III.C). We determine a feasible set of RTAs based on the remaining SOC of the eVTOLs, the minimum required SOC to reach the vertiport at these RTAs and the flight performance of the eVTOLs. The minimum RTA in the feasible set corresponds to the earliest possible time that the eVTOL can arrive at the vertiport. The maximum RTA in the feasible set is determined by the SOC of the eVTOL battery. The RTA obtained with the minimum energy consumption, which we refer to as the Estimated Time of Arrival (ETA), is the preferred arrival time of an eVTOL at the vertiport.

Having obtained a set of feasible RTAs for arriving eVTOLs, we next introduce a rolling-horizon optimisation model that sequences and schedules a set of G eVTOLs arriving at a vertiport such that the total time deviation from their ETAs, i.e., $\sum_{i \in G} |RTA_i - ETA_i|$, is minimised. The rolling-horizon [5, 26] consists of planning periods of $15min$ and a total planning horizon of $30min$, i.e., 2 planning periods (see Figure 3). In each planning horizon, we find the eVTOL RTAs that result in a minimal total time deviation from their ETAs. We freeze the RTAs of the eVTOLs in the first planning period, i.e., during the first $15min$. We also save the last RTA in this period, for each landing pad $RTA_{last,lp}(i), i \in \{A, B\}$. We further shift the planning horizon by $15min$ and optimise the arrival time of the remaining eVTOLs. We also ensure minimum separation between the time of the last eVTOL arrival in the previous planning period and the first eVTOL arrival in the next planning period.

Decision variables

We optimize the values of the following decision variables:

$$a^p = \begin{cases} 1, \text{ if eVTOL } p \text{ flies through approach fix } A, \\ 0, \text{ if eVTOL } p \text{ flies through approach fix } B, \end{cases} \quad \forall p \in G,$$

$$z^{pq} = \begin{cases} 1, \text{ if eVTOL } p \text{ and eVTOL } q \text{ fly through the same approach fix,} \\ 0, \text{ otherwise} \end{cases} \quad \forall p, q \in G,$$

$$s^{pq} = \begin{cases} 1, \text{ if eVTOL } p \text{ arrives prior to eVTOL } q, \\ 0, \text{ otherwise} \end{cases} \quad \forall p \in G, q \in [p-K, p+K], p \neq q, \text{where } K \in \mathbb{N}^+ \text{ is}$$

the maximum number of position shifts from the FCFS (First-Come-First-Served) arrival sequence [27].

Δt_e^p = Amount of time eVTOL p is scheduled beforeits $ETA^p(i)$, $i \in \{A, B\}$, i.e.,

$$ETA^p(i) - RTA^p(i), \qquad \forall p \in G, \ \Delta t_e^p \geq 0,$$

Δt_l^p = Delay assigned to eVTOL p in shallow descent,i.e, amount of time eVTOL p is scheduled after its $ETA^p(i)$, $i \in \{A, B\}$, i.e. , $RTA^p(i) - ETA^p(i), \forall p \in G,\ \Delta t_l^p \geq 0$,

$\Delta t_{l,h}^p$ = Delay assigned to eVTOL p in hover atdistance $R + r$ from the vertiport, i.e, amount of time eVTOL p is scheduled after its $ETA^p(i), i \in \{A, B\}$, i.e., $RTA^p(i) - ETA^p(i), \forall p \in G,\ 0 \leq \Delta t_{l,h}^p \leq \Delta t_{l,h,max}^p$, where $\Delta t_{l,h,max}^p$ is determined from the remaining battery SOC.

Objective function

The total time deviations from the ETAs of the eVTOLs arriving at the vertiport is minimized, i.e.:

$$\min \sum_{p \in G} c_e^p \cdot \Delta t_e^p + c_l^p \cdot \Delta t_l^p + c_{l,af}^p \cdot a^p \cdot (\Delta t_{l,A}^p - \Delta t_{l,B}^p) + c_{l,h}^p \cdot \Delta t_{l,h}^p, \text{ where} \tag{10}$$

$$\Delta t_{l,i}^p = \max\left(0, (ETA^p(i) + T_t^p(i) - ETA^p(j) - T_t^p(j))\right) \forall i, j \in \{A, B\}, i \neq j. \tag{11}$$

The first term in Eq. (10) penalises the amount of time eVTOLs arrive at the vertiport before their ETA. The second term penalises the delay assigned to eVTOLs in shallow descent. The third term penalises the additional flight time resulting from selecting an approach fix i, $i \in \{A, B\}$, which needs more time to reach, i.e., requires a longer arrival trajectory, than the other approach fix j, $j \in \{A, B\}$, $i \neq j$. The delay resulting from choosing an approach fix, i.e., $\Delta t_{l,i}^p$, $i \in \{A, B\}$, is calculated using Eq. (11), where $T_t^p(i)$ is the flight time between the approach fix i, $i \in \{A, B\}$ and the vertiport. The fourth term penalises the time the eVTOL spends hovering at distance $R + r$ from the vertiport. Further, $c_e^p, c_l^p, c_{l,af}^p, c_{l,h}^p$ are the cost coefficients corresponding to the four penalty terms above, where $c_e^p, c_l^p, c_{l,af}^p, c_{l,h}^p$ are derived from the power required to absorb the assigned time deviation of an eVTOL from its ETA.

Constraints

We require the following set of constraints to be satisfied:

$$s^{pq} + s^{qp} = 1, \forall p, q \in G \tag{12}$$

$$z^{pq} = z^{qp}, \forall p, q \in G \tag{13}$$

$$z^{pq} \geq a^p + a^q - 1, \forall p, q \in G, p \neq q \tag{14}$$

$$z^{pq} \geq -a^p - a^q + 1, \forall p, q \in G, p \neq q \tag{15}$$

$$z^{pq} \leq \frac{1}{2}a^p - \frac{1}{2}a^q + 1, \forall p, q \in G, p \neq q \tag{16}$$

$$z^{pq} \leq -\frac{1}{2}a^p + \frac{1}{2}a^q + 1, \forall p, q \in G, p \neq q \tag{17}$$

$$RTA_e^p \leq RTA^p \leq RTA_l^p, \forall p \in G \tag{18}$$

$$RTA^p \geq RTA^q + \Delta t_{sep}^{qp} \cdot z^{qp} - M^{pq} \cdot s^{pq}, \forall p, q \in G, p \neq q \tag{19}$$

$$RTA^p(i) \geq RTA^q(i) + \Delta t_{sep}^{qp} \cdot z^{qp} - M^{pq} \cdot s^{pq}, \forall p, q \in G, p \neq q, i \in \{A, B\} \tag{20}$$

in which

$$RTA_e^p = a^p \cdot RTA_{e,lp}^p(A) + (1 - a^p) \cdot RTA_{e,lp}^p(B) \tag{21}$$

$$M^{pq} = RTA_l^q + \Delta t_{l,h,max}^p + \Delta t_{sep}^{qp} - \min\left(RTA_{e,lp}^p(A),\ RTA_{e,lp}^p(B)\right) \tag{22}$$

$$RTA_{e,lp}^p(i) = \max\left(RTA_{last,lp}(i) + \Delta t_{sep}^{pq}, RTA_e^p(i) + T_t^p(i)\right), \forall i \in \{A, B\} \tag{23}$$

$$RTA^p = a^p \cdot \left(RTA^p(A) + T_t^p(A)\right) + (1 - a^p) \cdot \left(RTA^p(B) + T_t^p(B)\right) \tag{24}$$

$$RTA^p(i) = ETA^p(i) + \Delta t_l^p - \Delta t_e^p + \Delta t_{l,h}^p, \forall i \in \{A, B\}. \tag{25}$$

Constraint (12) ensures that either eVTOL p follows eVTOL q or eVTOL q follows eVTOL p. Equation (13) ensures that if eVTOL p and q go through the same approach fix and to the same landing pad, the reverse is also true. Equation (14) and (15) further define $z^{pq} = 1$ if both eVTOL p and q use approach fix A and B, respectively. Equation (16) and (17) define $z^{pq} = 0$ if eVTOLs p and q fly through different approach fixes. The feasible set of RTAs for landing at the vertiport is described in (18). The latest RTA_l^p results from the battery model (see Section III.C), while the earliest possible time of arrival RTA_e^p is computed by Eq. (21). Here, $RTA_{e,lp}^p(i)$ is the earliest possible landing time of eVTOL p arriving through approach fix i and thus at landing pad i, $i \in \{A, B\}$. This is derived from the flight performance model (see Section III.B). Equations (19) and (20) ensure a time-based separation of at least Δt_{sep}^{qp} only if eVTOL p follows eVTOL q at the same approach fix and, thus, the same landing pad. We consider variable M^{pq}, defined in Eq. (22), which ensures that the time separation between 2 eVTOLs is enforced only when $s^{pq} = 0$, i.e., when eVTOL p

arrives at the vertiport after eVTOL q. Equation (23) shows the earliest possible time to arrive at the vertiport based on the last eVTOL arrival time, $RTA_{last,lp}$, in the previous planning period. Equations (24) and (25) define the RTA for eVTOL p at the selected vertiport landing pad and at approach fix A or B, respectively.

E. eVTOL arrival demand model

We consider the eVTOL arrival demand model introduced in [8], where a prediction for an eVTOL arrival demand distribution over a day is provided for the hub vertiport in an envisioned hexagonal vertiport network of Houston, TX, USA. In [8], the distribution of arrivals is determined as the sum of 3 normal distributions: $N(8, 2)$ and $N(16, 2)$ corresponding to commuter rush hour peaks at 8:00AM and 4:00PM, respectively, and $N(12, 6)$ corresponding to daytime commuter travel. The obtained distribution (see Figure 4) is normalised to a cumulative distribution and scaled by coefficient $M_4 = 8500$ [8].

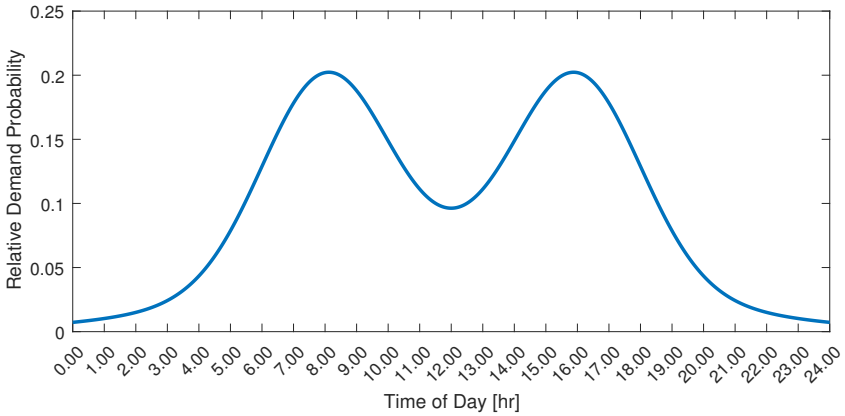

Fig. 4 Demand probability distribution function for eVTOL arrivals at a hub vertiport [8].

Using the probability distribution function in [8] for eVTOL arrivals at the hub vertiport, we estimate $\lambda(t)$, the number of arrivals in hour $t, t \in \{0, 1, \ldots, 24\}$. Further, we consider an inhomogeneous Poisson process with rate $\lambda(t)$ to generate eVTOL inter-arrival times at the vertiport. Moreover, based on the hexagonal vertiport network structure in [8], we assume that the eVTOLs start their arrival trajectory from one of 6 equally spaced, origin points on a circle of radius $R + r$ (see Figure 5). Each eVTOL has probability $1/6$ of originating from one of the 6 origin points on the circle.

Now, let an eVTOL $p + 1$ arriving at an approach fix i, $i \in \{A, B\}$ be preceded by eVTOL p. Then, the expected time of arrival of eVTOL $p + 1$ at an approach fix i, $ETA(i)^{p+1}$, is determined in Eq. (26), where S is the inter-arrival time between eVTOL $p + 1$ and eVTOL p, and is $\Delta t^p_{l,i}$ the additional flight time due to selecting approach fix i, which results in a longer arrival trajectory than selecting the other approach fix (see also Eq. (11)).

$$ETA(i)^{p+1} = ETA(i)^p + S + \Delta t^p_{l,i}, \tag{26}$$

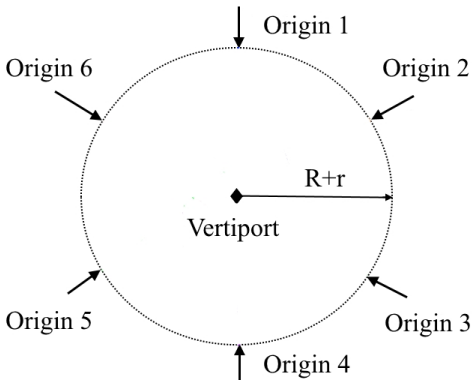

Fig. 5 Origin points for eVTOL arrivals at a hub vertiport.

where $S \sim exp(\lambda(t)),\ i \in \{A, B\}$.

Lastly, we assume that the initial SOC of an eVTOL p follows a normal distribution $N(30, 5)$, where a mean initial SOC battery of 30% allows for all trajectories with an RTA in the feasible set of RTAs (see Section III.D) to be fulfilled.

IV. Results

In this section we present the arrival sequencing and scheduling results for an EHANG 184 [23]. In Section IV.A we illustrate the energy consumption achieved by EHANG 184 for various RTAs and shallow descents. In Section IV.B we show the arrival delay for EHANG 184 for a rolling-horizon arrival sequencing and scheduling for one day of operations. In Section IV.C we discuss the distribution of EHANG 184 delays based on Monte Carlo simulation of a 1-day operations demand.

A. Energy-optimal arrival trajectory for a single eVTOL

In this section we determine, using the GPOPS-II trajectory optimizer and the flight dynamics model in Section III.B, the energy optimal arrival trajectories for a given set of RTAs at a given approach fix. The cruise phase is performed at $500m$ altitude and $27.8m/s$ cruise speed [23]. The eVTOL arrival scheduling and sequencing is initiated at $R + r = 3900m$ distance from the vertiport (see Section III.A). A shallow descent is initiated between $3400m$ and $1000m$ from the vertiport at a constant horizontal velocity $V_h = 5.9m/s$ and variable vertical velocity V_x. After passing the approach fix, a horizontal flight phase is executed at velocity $V_h = 5.9m/s$ and a vertical flight phase at velocity $V_x = 2.9m/s$.

Figure 6 shows the energy-optimal eVTOL arrival trajectories for given RTAs at the approach fix, RTA_{af}. For a large RTA_{af}, the eVTOLs spend this large time flying a more shallow descent. An $RTA_{af} = 165s$ is the shortest possible time to reach an approach fix, given the flight performance of EHANG 184 [23]. For $165s \leq RTA_{af} \leq 525s$, the eVTOL is required to arrive at the double landing pad vertiport at $262s \leq RTA \leq 622s$ since the flight time between the approach fix and vertiport is $97s$. A trajectory with $RTA_{af} = 165s$ also corresponds to the minimum energy required

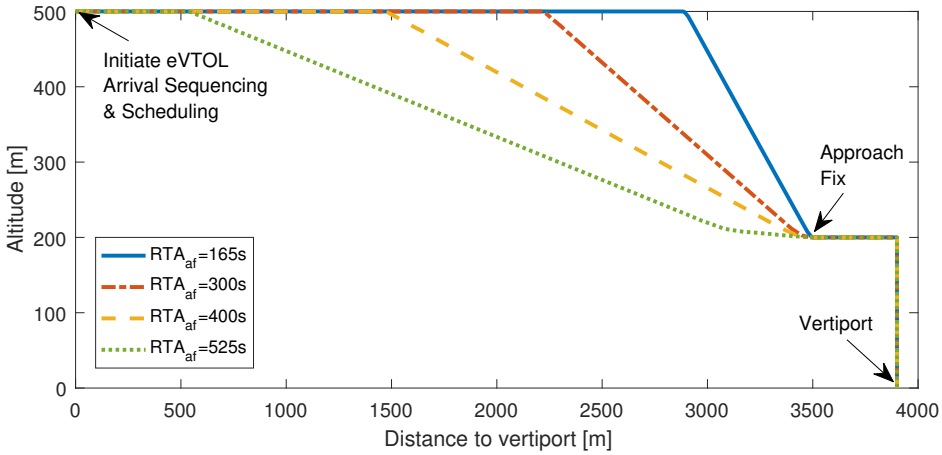

Fig. 6 EHANG 184 energy-optimal eVTOL arrival trajectory for different RTAs to approach fix.

to reach the approach fix. This trajectory with $RTA_{af} = 165s$ is used as a baseline trajectory to determine the eVTOLs ETAs at the vertiport, which are an input for the sequencing and scheduling model.

Figure 7 shows the SOC required to perform each of the trajectories in Figure 6, based on the battery model in Section III.C. We assume a battery capacity $Q = 5000Ahr$ and a nominal voltage $V_n = 12V$. Figure 7 shows, for instance, that for a remaining $SOC = 25\%$, the latest RTA at the approach fix is $RTA_{af} = 434s$. Thus, the maximum RTA at the vertiport is $RTA = 531s$.

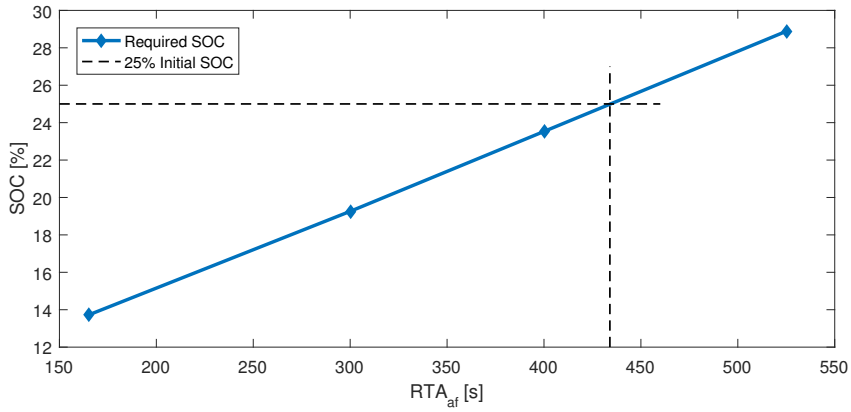

Fig. 7 Required SOC for different RTAs at approach fix.

B. A rolling-horizon arrival sequencing and scheduling for a 1-day eVTOL arrival demand

In this section we present the results of the rolling-horizon EHANG 184 arrival sequencing and scheduling optimisation model. We run the optimisation algorithm at the current time within a certain look-ahead planning period such as 5 and 10 minutes (see Table 1). After we calculate the RTAs for the flights in the current planning horizon, we

fix the RTAs and sequencing obtained up to this moment and move to next planning horizon. Next, we consider the new eVTOL arrivals, and run the optimisation algorithm again. We assume one day of operations demand, as introduced in Section III.E.

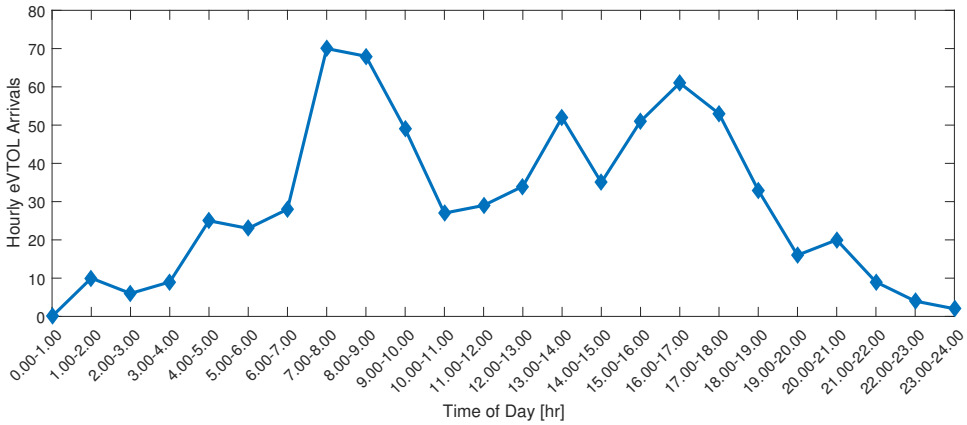

Fig. 8 Hourly eVTOL arrivals at the hub vertiport.

For the eVTOL arrival sequencing and scheduling optimisation model, we consider $c_e^p = 0$, $c_l^p = 28$, $c_{l,af}^p = 36$, $c_{l,h}^p = 42$, where $c_l^p = 28$ is the energy differential of a shallow descent trajectory that requires 1 additional second to be flown, i.e., $\frac{\Delta E}{\Delta t} = 28kW$, $c_{l,af}^p = 36$ is the power required to fly at cruise altitude and velocity, $c_{l,h}^p = 42$ is the power required to hover. Lastly, $c_e^p = 0$ since, for EHANG 184, the most energy-efficient trajectory, after using GPOPS-II, also corresponds to the earliest possible arrival time at the approach fix, i.e. $RTA_{af} = 165s$. We also assume $K = 2$ [27].

Figure 8 shows eVTOL arrivals over one day of operations, which are generated based on the demand model [8] in Section III.E.

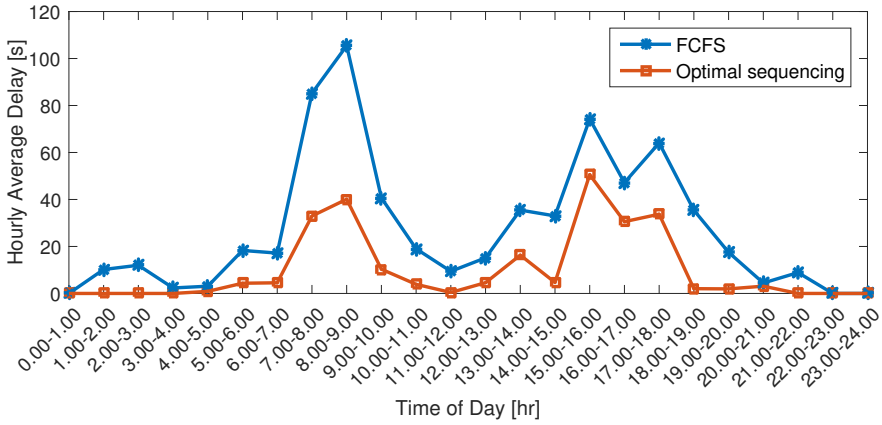

Fig. 9 Average eVTOL delay at the vertiport for one day.

We compared our arrival sequencing and scheduling algorithm with a baseline heuristic algorithm called first-come-

first-serve (FCFS). In Figures 9 and 10, we can observe that our algorithm dominates the FCFS through a 24-hour period in both reducing average delay and maximum delay. In air traffic control, the FCFS algorithm is a commonly used heuristic to mimic human controller's tactical decision making process. Specifically, in this application, the FCFS logic tries to first schedule the eVTOL aircraft to the minimum ETA between the ETA to fix A and the ETA to fix B. If this minimum ETA is the ETA to fix A and fix A is available (satisfying time separation constraint), then we schedule the eVTOL to fix A. If the minimum ETA is the ETA to fix B and fix B is available, then we schedule it to fix B. If the minimum ETA is the ETA to fix A and fix A is not available, but fix B is available, then we schedule it to fix B. If the minimum ETA is the ETA to fix B and B not available, but A is available, then we schedule it to fix A. In all cases, if the RTA exceeds the RTA upper bound according to the SOC, then we do not schedule this eVTOL. This corresponds to the case when, for instance, the eVTOL is redirected to another landing pad.

Figure 9 shows the average delay, i.e., $(RTA - ETA)$, imposed on eVTOLs arriving at the vertiport. Let us focus on discussing the result of our scheduling algorithm (the orange curve). In accordance to the demand peaks in Figure 8, the eVTOLs start to experience delays from early morning at 7:00AM until 9:00AM, with the highest average delay of $40s$. The eVTOL delays decrease significantly after 10:00AM. From 3:00PM, eVTOLs start experiencing higher delays again, with a highest average delay of $50s$. Figure 10 shows the maximum amount of delay that eVTOLs experience when arriving at the vertiport. Again, the highest delays occur around the peak demand hours, between 8:00AM and 9:00AM ($168s$) and between 3:00PM and 4:00PM ($309s$).

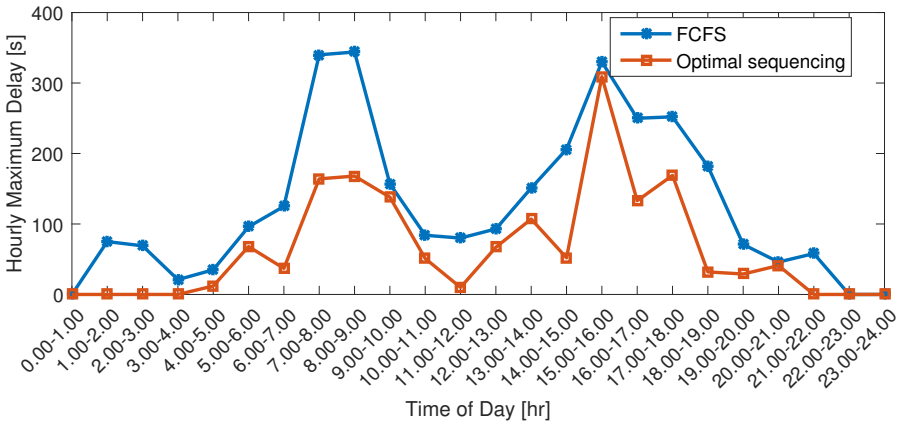

Fig. 10 Hourly maximum eVTOL delay at a double landing pad vertiport.

Table 1 shows both the computational time required to sequence and schedule, using a rolling-horizon approach, one day of operations, as well at the computational time for one planning horizon only. The results are obtained using CPLEX LP Solver extension of MATLAB on a computer with Intel CORE i7 processor. Table 1 shows that the required computational time is significantly high for a planning horizon of $15min$ or more. The use of short planning periods is, however, suitable for on-demand urban air mobility, where demand for eVTOLs occurs ad-hoc during the day.

Table 1 Computational time for the rolling-horizon eVTOL arrival sequencing and scheduling problem.

Length planning period [*min*]	**5**	**10**	**15**	**20**
Average computational time per planning horizon [s]	5.7	76	190	510

Figure 11 shows the impact of the minimum time separation between consecutive arrivals at the vertiport on the delay experienced by the eVTOLs. Increasing the time separation from 90s to 100s shows that, during peak demand hours around 8:00AM and 4:00PM, the eVTOL delays increase by up to 75%. In contrast, a time separation of 60s results in eVTOL delay of at most 10s, even during peak demand hours. Thus, designing eVTOLs for low time separation requirements is beneficial for on-time operations.

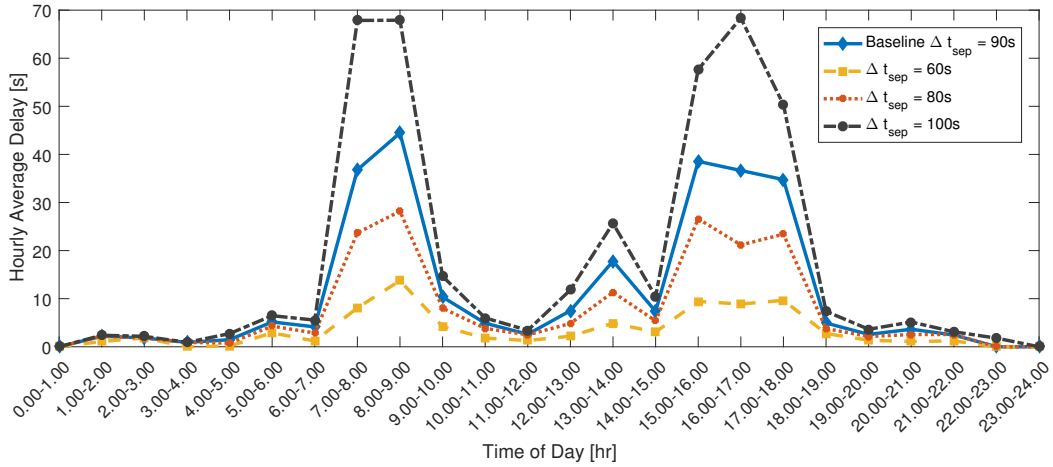

Fig. 11 Average eVTOL delay at a double landing pad vertiport - various minimum time separations.

In Figure 12, the performance of the scheduling model in terms of hourly expected delays is shown for different scaling coefficient M_4 of the eVTOL demand (see Section III.E). The results show that, for an increase of 10% in the scaling coefficient, i.e., $M_4 = 9350$, the expected delay during peak hours is almost double, compared with the baseline demand model with $M_4 = 8500$. The impact on delay is less for a decrease of 10% in the scaling coefficient, i.e., $M_4 = 7650$.

C. Monte Carlo simulation of eVTOL operations demand

We perform a Monte Carlo simulation of the demand of eVTOL operations (see Section III.E [8]) and evaluate the distribution of eVTOL delays. In particular, we consider that eVTOLs arrive at an area of radius 3900m around the vertiport according to a stochastic process. Also, the initial SOC of the batteries is assumed to follow a Gaussian distribution. For computational purposes, we evaluate two demand periods only: i) a peak demand period between 7:30AM to 8:30AM and ii) an off-peak demand period during noon time, from 11:30AM-12:30PM, when half as many

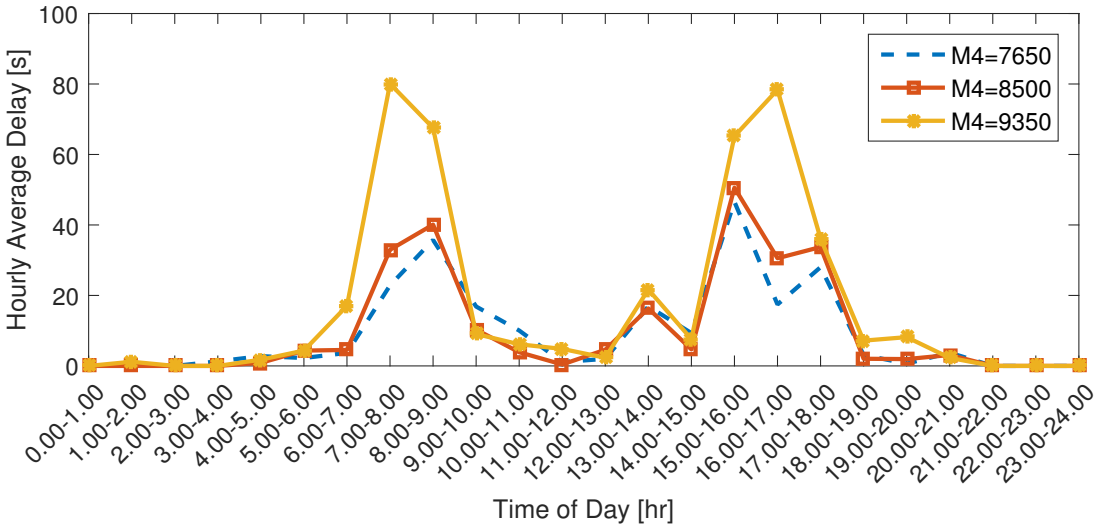

Fig. 12 Average eVTOL delay at a double landing pad vertiport - various coefficients of the eVTOL demand model.

eVTOL arrivals as in the peak period are expected to occur (see Figure 4).

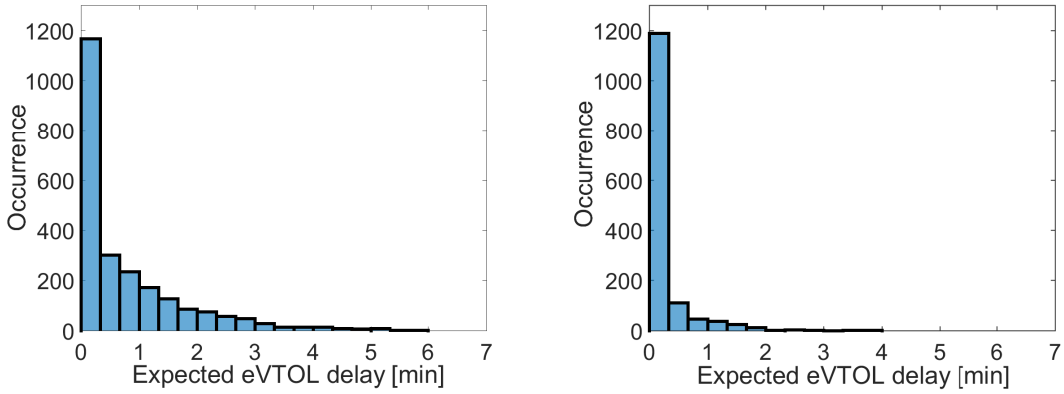

(a) Peak hour 7:30AM-8:30AM. **(b) Off-peak hour 11:30AM-12:30PM.**

Fig. 13 Distribution of eVTOL delay for eVTOLs arriving at a double landing pad vertiport.

Figure 13 and Figure 15 show that in off-peak periods, up to 94% of the arriving eVTOLs experience at most $1min$ delay. However, in the peak period, only 72% of the arriving eVTOLs experience at most $1min$ delay, with 24% of the eVTOLs having a delay of $1-3min$.

Figure 14 shows the distribution on the eVTOL arrival delays when considering a single and a double landing pad vertiport, respectively. The eVTOL arrival sequencing and scheduling optimisation model for a vertiport with one landing pad has been considered in [15]. The model in [15] has been further extended by considering a rolling-horizon approach to determine an optimal eVTOL arrival schedule. Moreover, the model has been extended with the possibility

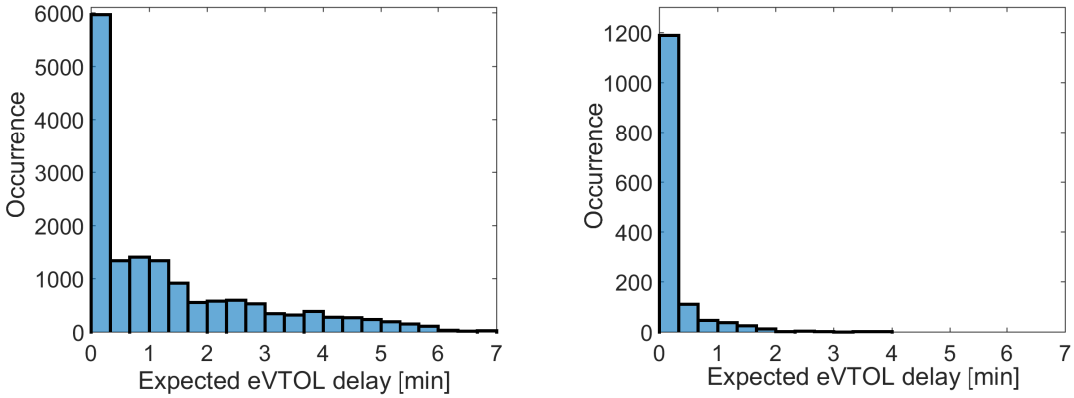

(a) Single landing pad vertiport **(b) Double landing pad vertiport.**

Fig. 14 Distribution of eVTOL delay during an off-peak hour 11:30AM-12.30PM.

for eVTOLs to hover at a distance $R + r$ from the vertiport.

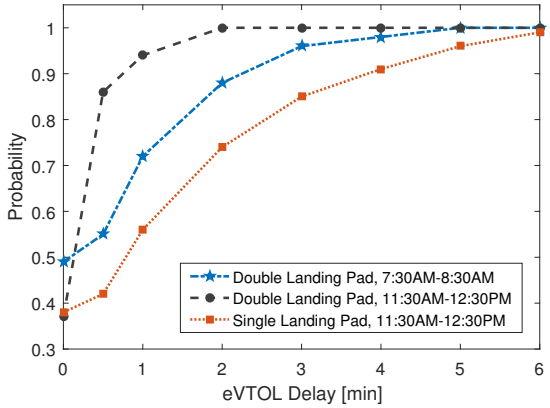

Fig. 15 Cumulative distribution function for eVTOL delay.

Figure 14 and Figure 15 shows that, during off-peak periods, having a double landing pad vertiport results in 94% of the arriving eVTOLs having at most $1min$ delay. However, having a single landing pad vertiport results only in 56% of the arrivals experiencing at most $1min$ delay, with 31% of the arrivals having a delay of $1 - 4min$. We note that for the peak hour 7:30AM-8:30AM, due to the high number of eVTOL arrivals, a single landing pad cannot accommodate the demand, thus we have not considered this case for simulation.

V. Discussion

This paper addresses the eVTOL arrival sequencing and scheduling at a vertiport terminal airspace such that the arrival delays are minimized. We consider potential shallow descent approaches to induce arrival delay. In turn, we generate required time of arrival (RTA) for the incoming aircraft to enforce such delays. We envision that this

arrival management model will complement pre-departure planning/scheduling models and strategic air traffic flow management models, while supporting safe and efficient urban air mobility operations.

In practice, we expect additional challenges for the eVTOL arrival process. Firstly, the arrival process is impacted by the capacity of the vertiport, and, in particular, by the eVTOL turnaround requirement. While we we consider arrival management to be one of the main priorities for urban air mobility operations, due to eVTOL battery constraints and envisioned high traffic densities in the terminal area, it remains a challenge to analyze together the arrival, turnaround and departure processes at a vertiport.

Secondly, further analysis of the potential demand for eVTOL operations throughout a day is needed to assess arrival scheduling algorithms. In particular, dedicated arrival heuristics should be developed to account for extreme demand values. For instance, in our paper we analyzed the FCFS heuristic, which is commonly used for arrival sequencing and scheduling of commercial aviation. Lastly, the design of contingency plans, such as, for instance, eVTOL vectoring or hovering, should be investigated together with arrival management algorithms.

VI. Conclusions

We consider a double landing pad vertiport where on-demand eVTOLs arrive. An optimal, rolling-horizon eVTOL sequencing and scheduling algorithm is proposed such that time deviations from a preferred arrival time are minimised. The optimisation problem is formulated as a mixed-integer linear program with constraints regarding the minimum time separation, electrical battery discharge, and vehicle dynamics. The discharge battery model, in particular, makes this arrival scheduling algorithm specially designed for eVTOL operations. We solve the sequencing and scheduling problem using a rolling-horizon approach for one day of operations, where the demand for operations corresponds to a hexagonal vertiport network in Houston, TX, USA. Our proposed sequencing and scheduling algorithm has arrival route selection capability. The algorithm outputs landing time slots (or RTAs) for all arriving eVTOLs to achieve minimum total delay. We determine the distribution of delays imposed on the arriving eVTOLs at the vertiport. We show that a double landing pad vertiport is able to accommodate the demand both in off-peak and peak hours, with eVTOLs average delays up to $50s$ in peak hours.

Future work includes (1) exploring other heuristics to achieve near real-time, sub-optimal solutions under high eVTOL demands, (2) design of terminal airspace and estimation of vertiport capacities, (3) accounting for uncertainties with respect to the eVTOL flight performance, and (4) investigating other delay absorption concepts such as ground delay at the departure vertiport, hovering and vectoring.

References

[1] Polaczyk, N., Trombino, E., Wei, P., and Mitici, M., "A Review of Current Technology and Research in Urban On-Demand Air Mobility Applications," *8th Biennial Autonomous VTOL Technical Meeting and 6th Annual Electric VTOL Symposium*, 2019.

[2] Uber Elevate, "Fast-Forwarding to a Future of On-Demand Urban Air Transportation," Tech. rep., Uber Elevate Whitepaper, 2016.

[3] Guérert, C., Prins, C., and Sevaux, M., *Applications of Optimization with XPress-MP*, Dash Optimization Ltd., 2000.

[4] Pawelek, A., Lichota, P., Dalmau, R., and Prats, X., "Arrival Traffic Synchronisation with Required Time of Arrivals for Fuel-efficient Trajectory," *Proceedings of the 17th ATIO-AIAA Aviation Technology, Integration, and Operations Conference*, 2017, pp. 1–14.

[5] Hu, X., and Chen, W., "Genetic Algorithm Based on Receding Horizon Control for Arrival Sequencing and Scheduling," *Engineering Applications of Artificial Intelligence*, Vol. 18, No. 5, 2005, pp. 633–642.

[6] Vascik, P., and Hansman, J., "Constraint Identification in On-Demand Mobility for Aviation through an Exploratory Case Study of Los Angeles," *Proceedings of 17th AIAA Aviation Technology, Integration, and Operations Conference*, 2017, pp. 1–25.

[7] Alonso, J., Arneson, H., Melton, J., Vegh, M., Walker, C., and Young, L., "System-of-Systems Considerations in the Notional Development of a Metropolitan Aerial Transportation System," Tech. rep., Stanford University and NASA Ames Research Center, 2017.

[8] Kohlman, L., and Patterson, M., "System-Level Urban Air Mobility Transportation Modeling and Determination of Energy-Related Constraints," *Proceedings of Aviation Technology, Integration, and Operations Conference*, 2018, p. 3677.

[9] Olive, X., and Morio, J., "Trajectory clustering of air traffic flows around airports," *Aerospace Science and Technology*, Vol. 84, 2019, pp. 776–781.

[10] Bennell, J. A., Mesgarpour, M., and Potts, C. N., "Airport Runway Scheduling," *4OR - A Quarterly Journal of Operations Research*, Vol. 9, No. 2, 2011, p. 115.

[11] Ozgur, M., and Cavcar, A., "0–1 integer programming model for procedural separation of aircraft by ground holding in ATFM," *Aerospace science and technology*, Vol. 33, No. 1, 2014, pp. 1–8.

[12] Andreeva-Mori, A., Suzuki, S., and Itoh, E., "Rule derivation for arrival aircraft sequencing," *Aerospace Science and Technology*, Vol. 30, No. 1, 2013, pp. 200–209.

[13] Wu, Y., Sun, L., and Qu, X., "A sequencing model for a team of aircraft landing on the carrier," *Aerospace Science and Technology*, Vol. 54, 2016, pp. 72–87.

[14] Bosson, C., and Lauderdale, T., "Simulation Evaluations of an Autonomous Urban Air Mobility Network Management and Separation Service," *Proceedings of Aviation Technology, Integration, and Operations Conference*, 2018, p. 3365.

[15] Kleinbekman, I., Mitici, M., and Wei, P., "eVTOL Arrival Sequencing and Scheduling for On-Demand Urban Air Mobility," *Proceedings of Digital Aviation Systems Conference*, 2018.

[16] Cuong Chi, G., Bole, B., Hogge, E., Vazquez, S., Daigle, M., Celaya, J., Weber, A., and Goebel, K., "Battery Charge Depletion Prediction on an Electric Aircraft," *Proceedings of the Annual Conference of the Prognostics and Health Management Society*, 2013, pp. 1–11.

[17] Bole, B., Daigle, M., and Gorospe, G., "Online Prediction of Battery Discharge and Estimation of Parasitic Loads for an Electric Aircraft," *Proceedings of the European Conference on the prognostics and health management society*, Vol. 2, 2014, p. 5S2P.

[18] Alnaqeb, A., Li, Y., Lui, Y., Pradeep, P., Wallin, J., Hu, C., Hu, S., and Wei, P., "Online Prediction of Battery Discharge and Flight Mission Assessment for Electrical Rotorcraft," *Proceedings of AIAA Aerospace Sciences Meeting*, 2018, p. 2005.

[19] Plett, G., *Equivalent-Circuit Methods*, Battery Management Systems, Vol. II, Artech House, 2016.

[20] Goodrich, K., and Barmore, B., "Exploratory Analysis of the Airspace Throughput and Sensitivities of an Urban Air Mobility System," *Proceedings of Aviation Technology, Integration, and Operations Conference*, 2018, p. 3364.

[21] Pradeep, P., and Wei, P., "Energy Efficient Arrival with RTA Constraint for Urban eVTOL Operations," *Proceedings of AIAA Aerospace Sciences Meeting*, 2018, pp. 1–13.

[22] Erzberger, H., and Itoh, E., "Design Principles and Algorithms for Air Traffic Arrival Scheduling," Tech. rep., NASA Ames Research Center, California, USA and Electronic Navigation Research Institute, Tokyo, Japan, 2014.

[23] EHANG184, "EHANG184 autonomous aerial vehicle specs," `http://www.ehang.com/ehang184/specs/`, 2018. Accessed March-2018.

[24] Johnson, W., *Rotorcraft Aeromechanics*, Cambridge University Press, 2013.

[25] Patterson, M., and Rao, A., "GPOPS-II: A MATLAB Software for Solving Multiple-Phase Optimal Control Problems Using hp-Adaptive Gaussian Quadrature Collocation Methods and Sparse Nonlinear Programming," *ACM Transactions on Mathematical Software (TOMS)*, Vol. 41, No. 1, 2014, pp. 1:1–1:37.

[26] Samà, M., D'Ariano, A., and Pacciarelli, D., "Optimal Aircraft Traffic Flow Management at a Terminal Control Area during Disturbances," *Procedia - Social and Behavioral Sciences*, Vol. 54, No. 1, 2014, pp. 460–469.

[27] Rodriguez-Diaz, A., Adenso-Diaz, B., and Gonzalez-Torre, P., "Minimizing deviation from scheduled times in a single mixed operation runway," *Computer Operations Research*, Vol. 78, 2017, pp. 193–202.